



HAL
open science

Charge conserving FE-PIC codes on general grids

Martin Campos Pinto, Sébastien Jund, Stéphanie Salmon, Eric Sonnendrücker

► **To cite this version:**

Martin Campos Pinto, Sébastien Jund, Stéphanie Salmon, Eric Sonnendrücker. Charge conserving FE-PIC codes on general grids. 2008. hal-00311429v1

HAL Id: hal-00311429

<https://hal.science/hal-00311429v1>

Preprint submitted on 21 Aug 2008 (v1), last revised 23 Dec 2009 (v3)

HAL is a multi-disciplinary open access archive for the deposit and dissemination of scientific research documents, whether they are published or not. The documents may come from teaching and research institutions in France or abroad, or from public or private research centers.

L'archive ouverte pluridisciplinaire **HAL**, est destinée au dépôt et à la diffusion de documents scientifiques de niveau recherche, publiés ou non, émanant des établissements d'enseignement et de recherche français ou étrangers, des laboratoires publics ou privés.

Charge conserving FE-PIC codes on general grids

Martin Campos Pinto, Sébastien Jund, Stéphanie Salmon and Eric Sonnendrücker
IRMA - Université Louis Pasteur and CNRS
CALVI - INRIA Lorraine *

August 17, 2008

Abstract

We develop a general mathematical framework for electromagnetic Particle-In-Cell (PIC) codes that can be used on structured as well as unstructured or hybrid grids. It can accommodate high order Maxwell solvers and arbitrary smoothing functions for the particles. Moreover, it includes an exact discrete continuity equation. We show that the lowest order version of our formulation corresponds on a rectangular grid to the traditional Cloud-In-Cell (CIC) version of the PIC method coupled to a Yee Maxwell solver and the Villasenor-Buneman charge deposition scheme.

1 Introduction

Particle-In-Cell (PIC) solvers have been a major tool for the understanding of the complex behavior of a plasma or a particle beam in many situations. An important issue for electromagnetic PIC solvers, where the fields are computed using Maxwell's equations, is the problem of discrete charge conservation. Indeed the charge and current densities ρ and \mathbf{J} computed numerically from the particles do not necessarily verify a discrete continuity equation, so that Maxwell's equations with these sources might be ill posed. Therefore electromagnetic PIC solvers need to deal with this issue, either by performing a field correction [5, 17, 18, 20] or by computing the current density in a specific way so as to enforce a discrete continuity equation [26, 13, 25]. The latter solution is strongly linked to the use of a Yee solver on a regular grid for Maxwell's equations. So it is not as widely applicable as the first method. However such a technique has the advantage compared to the other to be local and not to modify the electromagnetic field away from the source, which may generate causality errors for some applications. It is therefore important to develop charge conserving deposition algorithms that are more widely applicable than with the Yee solver on regular grids. Understanding how the Maxwell solver needs to behave in order to derive a discrete continuity equation is the aim of this paper.

Developing new efficient and reliable Maxwell solvers has been an area of intense research in the last 40 years and a good understanding of the reasons why some solvers work well and other do not has only been achieved recently with the concept of discrete differential forms (see [16] for a review). Let us now give a short overview of Finite Element (FE) solvers that have been developed for the 3D Maxwell equations in the Time Domain. These Finite Element methods are better adapted for complex geometries as they can be based on different computational elements (hexahedra, tetrahedra) which can be used to mesh efficiently complex geometries. Finite Elements adapted to Maxwell's equations, the so-called edge elements have been introduced by Nédélec [21]

*This work has been partially supported by Agence Nationale pour la Recherche under the grant ANR-06-CIS6-0013.

in 1980. Moreover the finite element methodology gives easy access to higher order methods which have proven useful recently for several applications [24, 8]. One of the drawbacks of these edge finite element methods for Time Domain computations is the need to solve a linear system at each time step. Therefore Mass-lumped elements have been introduced on squares, cubes and hexahedra [9, 14] for any order and on tetrahedra [12] for first and second order edge elements. Mass lumped nodal Finite Elements for a formulation of Maxwell’s equations keeping the divergence constraint and adding a Lagrange multiplier have also been developed [2].

We will see here how the framework of FE Maxwell solvers can be used to derive a discrete continuity equation by computing the current density \mathbf{J} in an adequate way. The paper is organized as follows. First we recall the 2D Maxwell equations and a variational formulation used for FE discretization with an emphasis on charge conservation issues. Then we propose a conforming FE discretization and examine the computation of the current density so as to find a formulation yielding an exact discrete continuity equation. We conclude with implementation issues, proposing a method for computing the discrete current density based on Gauss quadrature, so that the basic computations in the algorithm are the same as in a standard PIC code, the current only being evaluated at specific Gauss points on the particle’s trajectories. We also show that the lowest order version of our algorithm on a regular rectangular grid is exactly the Yee solver with a Villasenor-Buneman [26] current deposition.

All the theory and computations are performed in the 2D case, but can be extended in a straightforward manner to 3D.

2 The 2D Time domain Vlasov-Maxwell system

Schematically, the time evolution of a plasma breaks down into two simultaneous phenomena, as follows:

- the charged particles constituting the plasma generate an electromagnetic field,
- which in return affects the motion of the particles through the Lorentz force.

Now, although each phenomenon can be modeled by linear equations – namely Maxwell’s equations and Newton’s second law of dynamics – the coupling causes the resulting system to be highly nonlinear. Let us recall the equations in more details, and introduce some notations.

In a two dimensional domain Ω , the Maxwell system consists of two sets of decoupled equations: The first set, usually referred to as the Transverse Electric (TE) mode, involves the (E_x, E_y, B_z) components, whereas the second set (the Transverse Magnetic mode) involves the remaining components, namely (E_z, B_x, B_y) . Here we shall only consider the former, since the latter can be dealt with in a similar manner. Formally, the system reads

$$\partial_t \mathbf{E} - c^2 \mathbf{curl} B = -\frac{1}{\varepsilon_0} \mathbf{J} \quad (1)$$

$$\partial_t B + \mathbf{curl} \mathbf{E} = 0 \quad (2)$$

$$\mathbf{div} \mathbf{E} = \frac{\rho}{\varepsilon_0} \quad (3)$$

where $\mathbf{E} = (E_x, E_y)^T$ and $B = B_z$ denote the (relevant components of the) electric and magnetic fields. These are the unknowns of the system, whereas $\mathbf{J} = (J_x, J_y)^T$ and ρ respectively denote given current and charge density, seen as sources. As usual, the vector and scalar curl operators are given in 2d by

$$\mathbf{curl} \varphi := (\partial_y \varphi, -\partial_x \varphi)^T \quad \text{and} \quad \mathbf{curl} \varphi := \partial_x \varphi_y - \partial_y \varphi_x$$

for any scalar- and vector-valued functions φ and $\boldsymbol{\varphi} = (\varphi_x, \varphi_y)^T$, respectively (here and below, we shall try to denote vector-valued objects – such as functions, spaces or operators – with boldface characters). In order to have a well-posed Cauchy problem on Ω we shall later supplement (1)-(3) with initial and boundary conditions, see Section 3 below.

In the Vlasov model, the state of the plasma is represented by a time dependent *distribution function* f which, at any time t , is defined on the phase space $\hat{\Omega} := \{(\mathbf{x}, \mathbf{v}) \in \Omega \times \mathbb{R}^2\}$ consisting in all possible (physical) positions $\mathbf{x} = (x, y)$ and velocities $\mathbf{v} = (v_x, v_y)$ for the particles. For simplicity we shall only consider the evolution of one species of particles (namely, electrons) and assume the presence of a neutralizing uniform background ion distribution. Following from Newton's law, the non relativistic Vlasov equation reads

$$\partial_t f + \mathbf{v} \cdot \nabla_{\mathbf{x}} f + \frac{q}{m} \mathbf{F} \cdot \nabla_{\mathbf{v}} f = 0, \quad (4)$$

where q , m denote the charge and mass of an electron, and where the force term is given by the Lorentz law, i.e., $\mathbf{F} := \mathbf{E} + \mathbf{v} \times B = (E_x + v_y B, E_y - v_x B)^T$, which yields a first coupling between the Maxwell and Vlasov equations. The model is then completed by the second coupling which expresses the sources of (1)-(3) in terms of the distribution f , as follows.

$$\rho := q \int_{\mathbb{R}^2} f \, d\mathbf{v}, \quad \mathbf{J} := q \int_{\mathbb{R}^2} \mathbf{v} f \, d\mathbf{v}. \quad (5)$$

The following equivalence, which is well known, is at the heart of our study. Let us first state it in formal terms.

Theorem 2.1 (Charge conservation – formal level) *Given Ampere's law (1), the following properties are equivalent:*

- (i) *Gauss' law (3) is satisfied at any time t ,*
- (ii) *Gauss' law (3) is satisfied at the initial time, and the sources ρ , \mathbf{J} satisfy a charge conservation property (also called continuity equation)*

$$\partial_t \rho + \operatorname{div} \mathbf{J} = 0. \quad (6)$$

The proof is elementary (take the divergence of Ampere's law), but the corollary is of greatest importance: since ρ , \mathbf{J} *must* satisfy (6) for \mathbf{E} and B to be solutions to the Maxwell system, it suffices to satisfy Gauss' law at initial time for it to hold at any time. Of course, in order that there exist solutions to the Maxwell-Vlasov system, it is necessary that the sources given by (4)-(5) do indeed satisfy (6). Which clearly holds, since integrating the Vlasov equation (4) with respect to \mathbf{v} yields

$$\partial_t \rho = -q \int_{\mathbb{R}^2} \mathbf{v} \cdot \nabla_{\mathbf{x}} f \, d\mathbf{v} - \frac{q^2}{m} \int_{\mathbb{R}^2} \mathbf{F} \cdot \nabla_{\mathbf{v}} f \, d\mathbf{v} = -q \int_{\mathbb{R}^2} \operatorname{div}_{\mathbf{x}}(\mathbf{v} f) \, d\mathbf{v} - \frac{q^2}{m} \int_{\mathbb{R}^2} \operatorname{div}_{\mathbf{v}}(\mathbf{F} f) \, d\mathbf{v} = -\operatorname{div} \mathbf{J}$$

using the usual assumption that f vanishes as $\mathbf{v} \rightarrow \infty$. In the next sections we shall see how Theorem 2.1 translates into a discrete framework.

3 Variational formulations for the Maxwell system

3.1 Continuous formulation

In order to define a Finite Element approximation of the Maxwell system, let us now specify (1)-(3) in functional terms. Here we shall consider weak solutions and to do so we recall the following usual

notations (unless specified, we suppose in the sequel that all the spaces are defined on Ω , which is assumed polygonal and simply connected):

$$H^1 := \{v \in L^2 : \mathbf{grad} v \in \mathbf{L}^2\}, \quad H_0^1 := \{v \in H^1 : v|_{\partial\Omega} = 0\}, \quad H(\mathbf{curl}) := \{v \in L^2 : \mathbf{curl} v \in \mathbf{L}^2\}$$

$$\mathbf{H}(\mathbf{curl}) := \{\mathbf{v} \in \mathbf{L}^2 : \mathbf{curl} \mathbf{v} \in \mathbf{L}^2\} \quad \text{and} \quad \mathbf{H}_0(\mathbf{curl}) := \{\mathbf{v} \in \mathbf{H}_0(\mathbf{curl}) : \mathbf{v}|_{\partial\Omega} \times \mathbf{n} = 0\},$$

see e.g. [15] for more details about these spaces (note that in 2d, $H(\mathbf{curl})$ and H^1 coincide).

The usual way for defining weak solutions to the TE mode is then twofold: either weaken Ampere's law (i.e., interpret it with test functions in $\mathbf{H}_0(\mathbf{curl})$) and consider Faraday's law as it is (i.e., in L^2), or do the opposite, that is, interpret Faraday's law with test functions in $H_0(\mathbf{curl}) = H_0^1$ and Ampere's law with test functions in $\mathbf{H}_0(\mathbf{div})$. In this article we are mainly concerned with the first option, since the case of the second one is still not fully understood, see Remark 4.5. Let us recall that this first option is connected with the following exact sequence:

$$H_0^1 \xrightarrow{\mathbf{grad}} \mathbf{H}_0(\mathbf{curl}) \xrightarrow{\mathbf{curl}} L^2, \quad (7)$$

meaning that $\mathbf{grad}(H_0^1) \subset \mathbf{H}_0(\mathbf{curl})$, $\ker(\mathbf{curl}|_{\mathbf{H}_0(\mathbf{curl})}) = \mathbf{grad}(H_0^1)$ and $\mathbf{curl}(\mathbf{H}_0(\mathbf{curl})) \subset L^2$. It reads: find \mathbf{E} and B , such that

$$\mathbf{E}(0) = \mathbf{E}_0 \in \mathbf{H}_0(\mathbf{curl}) \quad \text{and} \quad B(0) = B_0 \in L^2, \quad \text{with} \quad \mathbf{div} \mathbf{E}_0 = \frac{\rho(0)}{\varepsilon_0} \quad (8)$$

and such that for almost every t in $(0, T)$, we have

$$\int_{\Omega} \varphi \partial_t \mathbf{E}(t) - c^2 \int_{\Omega} B(t) \mathbf{curl} \varphi = -\varepsilon_0^{-1} \int_{\Omega} \varphi \mathbf{J}(t) \quad \forall \varphi \in \mathbf{H}_0(\mathbf{curl}), \quad (9)$$

$$\int_{\Omega} \psi \partial_t B(t) + \int_{\Omega} \psi \mathbf{curl} \mathbf{E}(t) = 0 \quad \forall \psi \in L^2, \quad (10)$$

$$- \int_{\Omega} \mathbf{E}(t) \cdot \mathbf{grad} \phi = \varepsilon_0^{-1} \int_{\Omega} \phi \rho(t) \quad \forall \phi \in H_0^1. \quad (11)$$

Since the domain Ω is assumed polygonal and simply connected, we know that as long as the sources $\rho \in C^1(0, T; L^2)$, $\mathbf{J} \in C^1(0, T; L^2)$ satisfy the charge conservation property (6), there exists a unique solution to (8)-(11) with regularity

$$\mathbf{E} \in C^0(0, T; \mathbf{H}_0(\mathbf{curl})) \cap C^1(0, T; L^2) \quad \text{and} \quad B \in C^1(0, T; L^2) \quad (12)$$

(see e.g. [3, 11]).

Remark 3.1 *As the function $\mathbf{E}(t)$ belongs to \mathbf{L}^2 for all t , it is possible to define its divergence as a linear form on H_0^1 by setting*

$$\int_{\Omega} \mathbf{div} \mathbf{E}(t) \phi := - \int_{\Omega} \mathbf{E}(t) \cdot \mathbf{grad} \phi \quad \forall \phi \in H_0^1$$

(which coincides with the Green formula whenever $\mathbf{E}(t)$ is in $H(\mathbf{div})$, but can be seen as a definition for $\mathbf{E}(t) \in \mathbf{L}^2 \setminus H(\mathbf{div})$). In the functional analysis community, the dual space of H_0^1 is usually denoted H^{-1} , and relation (11) is equivalently rewritten as:

$$\mathbf{div} \mathbf{E}(t) = \varepsilon_0^{-1} \rho(t) \quad \text{in} \quad H^{-1}.$$

In the sequel we shall nevertheless ignore such extensions of differential operators, and stick to classical notations like in (11).

In this context, the “charge conservation” Theorem 2.1 takes the following form.

Theorem 3.1 (charge conservation – functional level) *Given (9) – i.e., Ampere’s law with test functions in $\mathbf{H}_0(\text{curl})$ – the following properties are equivalent:*

(i) Equation (11), i.e., Gauss’ law with test functions in H_0^1 :

$$-\int_{\Omega} \mathbf{E}(t) \cdot \mathbf{grad} \phi = \varepsilon_0^{-1} \int_{\Omega} \rho(t) \phi \quad \forall \phi \in H_0^1$$

holds for almost every time t ,

(ii) Equation (11) holds at the initial time only, and ρ, \mathbf{J} satisfy the charge conservation property with test functions in H_0^1 , i.e.,

$$\frac{d}{dt} \int_{\Omega} \rho(t) \phi - \int_{\Omega} \mathbf{J}(t) \cdot \mathbf{grad} \phi = 0 \quad \forall \phi \in H_0^1 \quad (13)$$

holds for almost every time t .

Proof. Again, the idea consists in ”taking the divergence” of Ampere’s law. In this context this can be done by writing (9) with $\varphi := \mathbf{grad} \phi$, where ϕ is arbitrary in H_0^1 . This makes sense since

$$\mathbf{grad} H_0^1 \subset \mathbf{H}_0(\text{curl}) \quad (14)$$

(which is an obvious part of the exact sequence property (7)), and yields, as $\mathbf{grad}(\text{curl}) \equiv \mathbf{0}$

$$\frac{d}{dt} \int_{\Omega} \mathbf{E} \cdot \mathbf{grad} \phi = -\varepsilon_0^{-1} \int_{\Omega} \mathbf{J} \cdot \mathbf{grad} \phi \quad \forall \phi \in H_0^1$$

using Green’s formula. Now, (11) clearly implies (13) :

$$\varepsilon_0^{-1} \frac{d}{dt} \int_{\Omega} \phi \rho(t) = -\frac{d}{dt} \int_{\Omega} \mathbf{E}(t) \cdot \mathbf{grad} \phi = \varepsilon_0^{-1} \int_{\Omega} \mathbf{J} \cdot \mathbf{grad} \phi \quad \forall \phi \in H_0^1.$$

Conversely (13) yields

$$\frac{d}{dt} \left(\int_{\Omega} \rho \phi + \varepsilon_0 \int_{\Omega} \mathbf{E} \cdot \mathbf{grad} \phi \right) = 0 \quad \forall \phi \in H_0^1,$$

which ends the proof. ■

3.2 Conforming Finite Element discretizations of Maxwell’s equations

Let now V_h^0, \mathbf{V}_h^1 and V_h^2 denote finite element spaces embedded into $H_0^1, \mathbf{H}_0(\text{curl})$ and L^2 , respectively (such as (19) or (20) below). Moreover, assume that \mathbf{J}_h, ρ_h are approximations to \mathbf{J}, ρ . The conforming finite element space (semi-) discretization of the system (9)-(11) reads: find $\mathbf{E}_h \in \mathbf{V}_h^1$ and $B_h \in V_h^2$ such that

$$\frac{d}{dt} \int_{\Omega} \mathbf{E}_h \varphi - c^2 \int_{\Omega} B_h \text{curl} \varphi = -\varepsilon_0^{-1} \int_{\Omega} \mathbf{J}_h \varphi \quad \forall \varphi \in \mathbf{V}_h^1 \quad (15)$$

$$\frac{d}{dt} \int_{\Omega} B_h \psi + \int_{\Omega} \psi \text{curl} \mathbf{E}_h = 0 \quad \forall \psi \in V_h^2 \quad (16)$$

$$-\int_{\Omega} \text{div} \mathbf{E}_h \cdot \mathbf{grad} \phi = \varepsilon_0^{-1} \int_{\Omega} \rho_h \phi \quad \forall \phi \in V_h^0, \quad (17)$$

which we again supplement with initial conditions, such as

$$\mathbf{E}_h(0) = \mathbf{\Pi}_h^1 \mathbf{E}_0 \in \mathbf{V}_h^1 \quad \text{and} \quad B_h(0) = \Pi_h^2 B_0 \in V_h^2, \quad (18)$$

with $\mathbf{\Pi}_h^1, \Pi_h^2$ denoting stable projectors on \mathbf{V}_h^1 and V_h^2 , respectively.

For sake of completeness, let us recall that a usual choice for the conforming finite element spaces is the first Nédélec family [21] corresponding to:

$$\begin{cases} V_h^0 = V_{h,p}^0 := \{q \in \mathcal{C}^0(\Omega) : q|_\kappa \in \mathbb{Q}_{p,p} \quad \forall \kappa \in \Omega_h\}, \\ \mathbf{V}_h^1 = \mathbf{V}_{h,p}^1 := \{\mathbf{q} = (q_x, q_y) \in \mathbf{H}_0(\text{curl}; \Omega) : \mathbf{q}|_\kappa \in \mathbb{Q}_{p-1,p} \times \mathbb{Q}_{p,p-1} \quad \forall \kappa \in \Omega_h\}, \\ V_h^2 = V_{h,p}^2 := \{q \in L^2(\Omega) : q|_\kappa \in \mathbb{Q}_{p-1,p-1} \quad \forall \kappa \in \Omega_h\}, \end{cases} \quad (19)$$

on structured meshes (i.e., when Ω_h consists of quadrangles); with $\mathbb{Q}_{p,p'} := \text{Span}\{(x, y) \rightarrow x^a y^b : 0 \leq a \leq p, 0 \leq b \leq p'\}$. In the case of unstructured meshes (i.e., when Ω_h consists of triangles), this family corresponds to:

$$\begin{cases} V_h^0 = V_{h,p}^0 := \{q \in \mathcal{C}^0(\Omega) : q|_\kappa \in \mathbb{P}_p \quad \forall \kappa \in \Omega_h\}, \\ \mathbf{V}_h^1 = \mathbf{V}_{h,p}^1 := \{\mathbf{q} = (q_x, q_y)^T \in \mathbf{H}_0(\text{curl}; \Omega) : \mathbf{q}|_\kappa \in (\mathbb{P}_{p-1})^2 \oplus \begin{pmatrix} y \\ -x \end{pmatrix} \tilde{\mathbb{P}}_{p-1} \quad \forall \kappa \in \Omega_h\}, \\ V_h^2 = V_{h,p}^2 := \{q \in L^2(\Omega) : q|_\kappa \in \mathbb{P}_{p-1} \quad \forall \kappa \in \Omega_h\}, \end{cases} \quad (20)$$

with $\mathbb{P}_p := \text{Span}\{(x, y) \rightarrow x^a y^b : 0 \leq a, b, a + b \leq p\}$ and $\tilde{\mathbb{P}}_p := \text{Span}\{(x, y) \rightarrow x^a y^{p-a} : 0 \leq a \leq p\}$. As is well known, these discrete spaces satisfy an exact sequence property

$$V_h^0 \xrightarrow{\mathbf{grad}} \mathbf{V}_h^1 \xrightarrow{\text{curl}} V_h^2, \quad (21)$$

which follows from the analogue property of their continuous counterparts, see (7). In fact the only non-trivial property to be checked is that $\ker(\text{curl}|_{\mathbf{V}_h^1}) = \mathbf{grad}(V_h^0)$. To do this, observe that for any $\boldsymbol{\varphi} = \mathbf{q} + \begin{pmatrix} y \\ -x \end{pmatrix} \tilde{q}$ with $\mathbf{q} \in (\mathbb{P}_{p-1})^2$, $\tilde{q} \in \tilde{\mathbb{P}}_{p-1}$ (i.e., in the case of unstructured meshes), one has

$$\text{curl } \boldsymbol{\varphi} = \text{curl } \mathbf{q} - (p+1)\tilde{q}.$$

Since $\text{curl } \mathbf{q}$ clearly belongs to \mathbb{P}_{p-2} , $\text{curl } \boldsymbol{\varphi} = 0$ yields $\tilde{q} = 0$, hence $\boldsymbol{\varphi} \in (\mathbb{P}_{p-1})^2$. Using this observation with the continuous exact sequence property, we find $\boldsymbol{\varphi} = \mathbf{grad } \phi$ for some $\phi \in \mathbb{P}_p$. Note that in the sequel we shall only need the embedding

$$\mathbf{grad } V_h^0 \subset \mathbf{V}_h^1, \quad (22)$$

which easily follows from (14) and the conformity of the spaces, as well as their polynomial definition. In this conforming Galerkin setting, the formal charge conservation Theorem 2.1 takes a form completely similar to Theorem 3.1.

Theorem 3.2 (charge conservation – semi-discrete level) *Given (15) – which can be seen as Ampere’s law with test functions in \mathbf{V}_h^1 – the following properties are equivalent:*

- (i) Equation (11) (which can be seen as Gauss’ law with test functions in V_h^0 , see Remark 3.1), i.e.,

$$-\int_{\Omega} \mathbf{E}_h(t) \cdot \mathbf{grad } \phi = \varepsilon_0^{-1} \int_{\Omega} \rho_h(t) \phi \quad \forall \phi \in V_h^0$$

holds for almost every time t ,

(ii) Gauss' law holds with test functions in V_h^0 at the initial time only, and ρ_h, \mathbf{J}_h satisfy the charge conservation property with test functions in V_h^0 , i.e.,

$$\frac{d}{dt} \int_{\Omega} \rho_h(t) \phi - \int_{\Omega} \mathbf{J}_h(t) \cdot \mathbf{grad} \phi = 0 \quad \forall \phi \in V_h^0 \quad (23)$$

holds for almost every time t .

Proof. Simply repeat the proof of Theorem (3.1), replacing every continuous space by its discrete counterpart – which is possible according to (22). ■

4 Fully discrete scheme for the Vlasov-Maxwell system

4.1 Particle solver for the Vlasov equation

Let us recall the main lines of the Particle in Cell (PIC) solver, in the context of a second order leap-frog time discretization (see e.g. [5] for a more detailed presentation).

- approximate the initial density f_0 by a finite sum of “macro-particles”, i.e., Dirac measures located at phase space positions $\{(\mathbf{x}_k^0, \mathbf{v}_k^0) : k = 1, \dots, N_{\text{part}}\}$,

$$f_0(\mathbf{x}, \mathbf{v}) \approx f_h^0 := \sum_{k=1}^{N_{\text{part}}} w_k \delta(\mathbf{x} - \mathbf{x}_k^0, \mathbf{v} - \mathbf{v}_k^0) \quad (24)$$

with corresponding weights w_k chosen in such a way that f_h^0 is a good approximation of f_0 .

- transport the particles following the explicit scheme

$$\frac{\mathbf{x}_k^{n+1} - \mathbf{x}_k^n}{\Delta t} = \mathbf{v}_k^{n+\frac{1}{2}}, \quad \frac{\mathbf{v}_k^{n+\frac{1}{2}} - \mathbf{v}_k^{n-\frac{1}{2}}}{\Delta t} = \frac{q}{m} \left(\mathbf{E}_h^n(\mathbf{x}_k^n) + \frac{1}{2} (\mathbf{v}_k^{n+\frac{1}{2}} + \mathbf{v}_k^{n-\frac{1}{2}}) \times B_h^n(\mathbf{x}_k^n) \right) \quad (25)$$

(here we assume that consistent velocities $\mathbf{v}_k^{-\frac{1}{2}}, k = 1, \dots, N_{\text{part}}$, have been defined).

Note the improper notations in (24) – where the right hand side is not a function but a (Radon) measure – used for sake of simplicity. In most practical situations however, the Dirac measures are replaced by local smooth “shape functions” S such as B-splines, hence the initial density f_0 is indeed approximated by a (smooth) function

$$f_0(\mathbf{x}, \mathbf{v}) \approx \sum_{k=1}^{N_{\text{part}}} w_k S(\mathbf{x} - \mathbf{x}_k^0, \mathbf{v} - \mathbf{v}_k^0).$$

Now, since this is essentially needed when the Maxwell system is approximated by a finite difference scheme, we shall essentially be interested in the simpler case where no smoothing is performed, i.e., where $S := \delta$.

Of course, it now remains to define the fully discrete fields \mathbf{E}_h^n and B_h^n , which is described in the following section.

4.2 The coupled solver and the discrete charge conservation theorem

In order to complete the global scheme, we consider an explicit second order leap frog discretization of (15)-(16): starting from (18), we define $\mathbf{E}_h^{n+1} \in \mathbf{V}_h^1$ and $B_h^{n+1/2} \in V_h^2$, $n \in \mathbb{N}$, by

$$\frac{1}{\Delta t} \int_{\Omega} (\mathbf{E}_h^{n+1} - \mathbf{E}_h^n) \cdot \boldsymbol{\varphi} - c^2 \int_{\Omega} B_h^{n+1/2} \operatorname{curl} \boldsymbol{\varphi} = -\varepsilon_0^{-1} \int_{\Omega} \mathbf{J}_h^{n+1/2} \cdot \boldsymbol{\varphi} \quad \forall \boldsymbol{\varphi} \in \mathbf{V}_h^1 \quad (26)$$

$$\frac{1}{\Delta t} \int_{\Omega} (B_h^{n+1/2} - B_h^{n-1/2}) \psi + \int_{\Omega} \psi \operatorname{curl} \mathbf{E}_h^n = 0 \quad \forall \psi \in V_h^2 \quad (27)$$

(see also the matrix formulation below), where for simplicity it is assumed that a consistent $B_h^{-1/2}$ has been defined for the first step.

The PIC method (25) is then usually coupled with the FE scheme (26)-(27) by setting $B_h^n := \frac{1}{2}(B_h^{n+1/2} + B_h^{n-1/2})$ on the one hand, and

$$\rho_h^n(\mathbf{x}) := \sum_{k=1}^{N_{\text{part}}} w_k S(\mathbf{x} - \mathbf{x}_k^n), \quad \mathbf{J}_h^{n+1/2}(\mathbf{x}) := \sum_{k=1}^{N_{\text{part}}} w_k \mathbf{v}_k^{n+1/2} S(\mathbf{x} - \mathbf{x}_k^{n+1/2}) \quad (28)$$

on the other hand (with $\mathbf{x}_k^{n+1/2} := \frac{1}{2}(\mathbf{x}_k^{n+1} + \mathbf{x}_k^n)$). Here S denotes the Dirac δ in the unsmoothed case or a smoothing function (often called shape function in the PIC literature) which is typically a B-spline. Again, let us mention that some smoothing is already performed via the FE basis function, so that additional smoothing is not strictly necessary, and generally not used, as opposite to the finite difference framework. In Figure 1 we have summarized the overall structure of the solver, with an emphasis on the ordering of the computations within every time step.

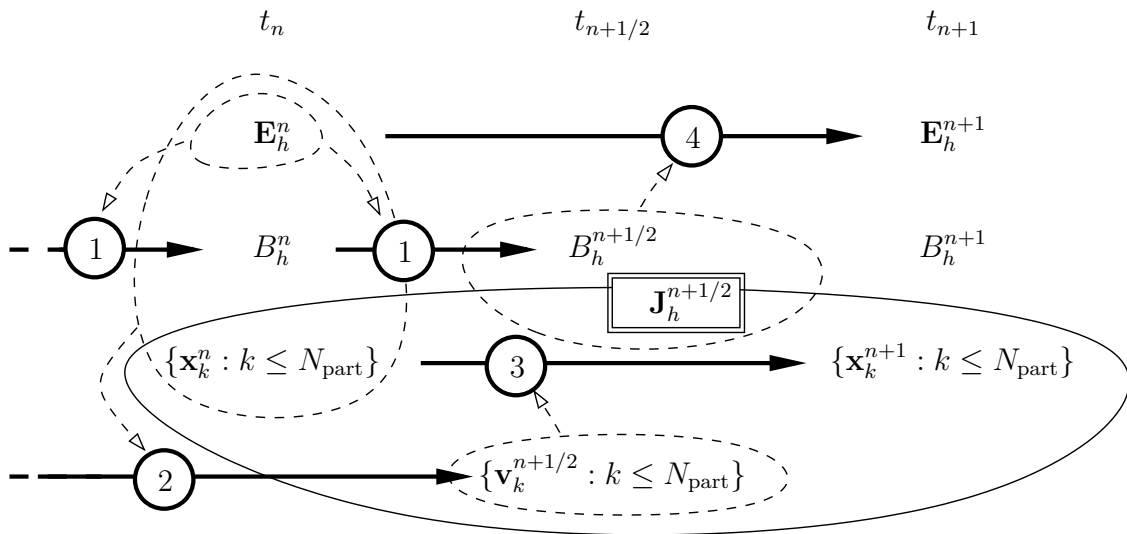


Figure 1: Overall view of the coupled FE-PIC scheme.

Remark 4.1 In the case where the PIC approximation is not smoothed, i.e., when $S = \delta$, the approximated current $\mathbf{J}_h^{n+1/2}$ is not an L^2 function. In order for the above variational formulation (26) of Ampere's law to still make sense, it is then necessary to replace every L^2 scalar product

$\int_{\Omega} \mathbf{J}_h^{n+1/2} \boldsymbol{\varphi}$, $\boldsymbol{\varphi} \in \mathbf{V}_h^1$ by classical duality pairings between Dirac measures and continuous functions, i.e.,

$$\langle \mathbf{J}_h^{n+1/2}, \boldsymbol{\varphi} \rangle = \sum_{k=1}^{N_{\text{part}}} w_k \mathbf{v}_k^{n+1/2} \langle \delta(\cdot - \mathbf{x}_k^{n+1/2}), \boldsymbol{\varphi} \rangle := \sum_{k=1}^{N_{\text{part}}} w_k \mathbf{v}_k^{n+1/2} \boldsymbol{\varphi}(\mathbf{x}_k^{n+1/2}).$$

Note that because the basis functions $\boldsymbol{\varphi}$ are only piecewise continuous, this only makes sense if the particle's positions \mathbf{x}_k^n are inside the cells (which we can always assume, up to rounding errors).

Now, as is well known – and we shall soon recall why –, defining the sources by (28) does not guarantee the conservation of the discrete charge. In particular, the associated discrete Gauss' law, see equation (29) below, is not satisfied *a priori* by the solution of (25)-(28). In order to circumvent this obstacle, different correction schemes have been introduced in the field solvers since the early 70s, such as the Boris correction [6], the Marder/Langdon method [18, 17], or the so-called generalized Maxwell formulation [2, 20] (see also [3] for an analysis of these formulations).

In order to understand why the above coupling is inconsistent, and propose a better one, we now rewrite the “charge conservation theorem” in the context of fully discrete FE-PIC schemes of arbitrary order.

Theorem 4.1 (charge conservation – fully discrete level) *Given the discrete Ampere law (26), the following are equivalent:*

(i) *the fully discrete Gauss law*

$$-\int_{\Omega} \mathbf{E}_h^n \cdot \mathbf{grad} \phi = \varepsilon_0^{-1} \int_{\Omega} \rho_h^n \phi \quad \forall \phi \in V_h^0 \quad (29)$$

holds at any time step n ,

(ii) *the discrete Gauss law (29) holds at the initial time step $n = 0$ only, and the discrete sources $\rho_h^n, \mathbf{J}_h^{n+1/2}$ satisfy the following discrete charge conservation property:*

$$\int_{\Omega} (\rho_h^{n+1} - \rho_h^n) \phi - \Delta t \int_{\Omega} \mathbf{J}_h^{n+1/2} \cdot \mathbf{grad} \phi = 0 \quad \forall \phi \in V_h^0 \quad \text{and } n \in \mathbb{N}. \quad (30)$$

Proof. Repeat the proof of Theorem 3.2, with divided differences in place of time derivatives. ■

Remark 4.2 *In the case where $S = \delta$, the above Theorem still makes sense if the L^2 scalar products involving sources are replaced by duality pairings, as described in Remark 4.1.*

4.3 A new formulation to ensure the conservation of charge

In the light of Theorem 4.1, it is now an easy task to see why the sources (28) fail to satisfy the discrete charge conservation, and hence the discrete Gauss law (29). Observe indeed that setting (i.e., interpolating)

$$\mathbf{v}_k(t) := \mathbf{v}_k^{n+1/2} \quad \text{and} \quad \mathbf{x}_k(t) := \mathbf{x}_k^n + (t - t_n) \mathbf{v}_k^{n+1/2} \quad \forall t \in [t_n, t_{n+1}],$$

and defining accordingly

$$\rho_h(t, \mathbf{x}) := \sum_{k=1}^{N_{\text{part}}} w_k S(\mathbf{x} - \mathbf{x}_k(t)) \quad \text{and} \quad \mathbf{J}_h(t, \mathbf{x}) := \sum_{k=1}^{N_{\text{part}}} w_k \mathbf{v}_k(t) S(\mathbf{x} - \mathbf{x}_k(t)),$$

we have (at least formally) $\int_{\Omega} (\rho_h^{n+1} - \rho_h^n) \phi = \int_{t_n}^{t_{n+1}} \left[\frac{d}{dt} \int_{\Omega} \rho_h(t) \phi \right] dt$. Now, for any $\phi \in V_h^0$ and any smooth shape function S , a straightforward computation and a Green formula yield

$$\begin{aligned} \frac{d}{dt} \int_{\Omega} S(\cdot - \mathbf{x}_k(t)) \phi &= - \int_{\Omega} [\mathbf{v}_k(t) \cdot \mathbf{grad} S(\cdot - \mathbf{x}_k(t))] \phi = - \int_{\Omega} [\operatorname{div}(\mathbf{v}_k(t) S(\cdot - \mathbf{x}_k(t)))] \phi \\ &= \int_{\Omega} \mathbf{v}_k(t) S(\cdot - \mathbf{x}_k(t)) \cdot \mathbf{grad} \phi, \end{aligned}$$

in particular $\frac{d}{dt} \int_{\Omega} \rho_h(t) \phi$ is bounded, hence we can sum over every particle and compute

$$\int_{\Omega} (\rho_h^{n+1} - \rho_h^n) \phi = \int_{t_n}^{t_{n+1}} \left[\sum_{k=1}^{N_{\text{part}}} w_k \frac{d}{dt} \int_{\Omega} S(\cdot - \mathbf{x}_k(t)) \phi \right] dt = \int_{t_n}^{t_{n+1}} \left[\int_{\Omega} \mathbf{J}_h(t) \cdot \mathbf{grad} \phi \right] dt. \quad (31)$$

Remark 4.3 If $S = \delta$, the L^2 scalar products must be replaced by duality pairings between Dirac measures and continuous functions, i.e., for any $\phi \in V_h^0$ we have

$$\langle \rho_h(t), \phi \rangle = \sum_{k=1}^{N_{\text{part}}} w_k \langle \delta(\cdot - \mathbf{x}_k(t)), \phi \rangle = \sum_{k=1}^{N_{\text{part}}} w_k \phi(\mathbf{x}_k(t)).$$

Because this is a Lipschitz function of t , with derivative $\frac{d}{dt} \langle \rho_h(t), \phi \rangle = \sum_{k=1}^{N_{\text{part}}} w_k \mathbf{v}_k(t) \cdot \mathbf{grad} \phi(\mathbf{x}_k(t))$, the principle used in the above computation applies again, i.e., we can compute

$$\langle \rho_h^{n+1} - \rho_h^n, \phi \rangle = \int_{t_n}^{t_{n+1}} \sum_{k=1}^{N_{\text{part}}} w_k \mathbf{v}_k(t) \cdot \mathbf{grad} \phi(\mathbf{x}_k(t)) = \int_{t_n}^{t_{n+1}} \langle \mathbf{J}_h(t), \mathbf{grad} \phi \rangle. \quad (32)$$

Unless \mathbf{J}_h is affine on (t_n, t_{n+1}) the above relation has no reason to coincide with the desired (30), which is the reason why the FE-PIC scheme (25)-(28) fails to ensure both the charge conservation and the Gauss law. The *good news* is: we now have an obvious cure for the lack of consistency. Let us state it as our main theorem (and refer to section 5.2 for a practical algorithm in the case where no regularization is performed, i.e., $S = \delta$).

Theorem 4.2 (Consistent coupling for FE-PIC schemes) *The numerical solutions to the FE-PIC scheme (25)-(27) complemented with the new source definitions*

$$\rho_h^n(\mathbf{x}) := \sum_{k=1}^{N_{\text{part}}} w_k S(\mathbf{x} - \mathbf{x}_k^n), \quad \bar{\mathbf{J}}_h^{n+\frac{1}{2}}(\mathbf{x}) := \sum_{k=1}^{N_{\text{part}}} w_k \mathbf{v}_k^{n+\frac{1}{2}} \frac{1}{\Delta t} \int_{t_n}^{t_{n+1}} S(\mathbf{x} - \mathbf{x}_k(t)) dt \quad (33)$$

(with $\mathbf{x}_k(t) := \mathbf{x}_k^n + (t - t_n) \mathbf{v}_k^{n+1/2}$ for $t \in [t_n, t_{n+1}]$) do satisfy the discrete charge conservation property (30), hence the discrete Gauss law (29) too, provided the latter holds at the initial time step. In other terms, defining the current appearing in the discrete Maxwell system as a time average $\frac{1}{\Delta t} \int_{t_n}^{t_{n+1}} \mathbf{J}_h(t) dt$ in place of the instantaneous value $\mathbf{J}_h(t_{n+1/2})$ yields a consistent coupling.

Remark 4.4 By observing that (31) – or (32) in the case where $S = \delta$ – holds not only for ϕ in V_h^0 but for any ϕ in $C_c^\infty(\Omega)$ (the space of infinitely differentiable functions with compact support in Ω), we see that

$$\rho_h^{n+1} - \rho_h^n + \Delta t \operatorname{div} \bar{\mathbf{J}}_h^{n+\frac{1}{2}} = 0 \quad (34)$$

holds in distribution's sense. In particular, (34) holds in a point-wise sense (on Ω) when S is a continuous function, since in this case ρ_h^n is also continuous (note that this also establishes the continuity of $\operatorname{div} \bar{\mathbf{J}}_h^{n+1/2}$).

Remark 4.5 (the case of the second formulation) *Let us emphasize the following interpretation of (34): the sources given by (33) do satisfy a charge conservation property which is independent of the given formulation of Maxwell's equations, and hence intrinsic. In particular, one would be tempted to define the sources in the same way when considering the second formulation mentioned in Section 3.1. Unfortunately this does not lead to the proper discrete Gauss law, i.e., the analogous of (29) for the corresponding spaces.*

5 Implementation issues

This section is devoted to discuss some important aspects of the implementation. In particular, we shall describe a simple algorithm for computing the new (consistent) right hand side involved in the matrix formulation of the Maxwell solver (26)-(27), recall mass lumping techniques for structured meshes and show that our formulation coincides with the method of Villasenor and Buneman for first order elements and is in some way a generalization for high order and unstructured grids of this method.

5.1 Matrix formulation of the Maxwell solver

Let us now consider that $\Phi_h^1 = \{\varphi_i^1 : i = 1, \dots, N_h^1\}$, $\Psi_h^2 = \{\psi_i^2 : i = 1, \dots, N_h^2\}$ are given bases of the FE spaces \mathbf{V}_h^1 and V_h^2 , respectively, and that $\{\sigma_i^1 : i = 1, \dots, N_h^1\}$, $\{\sigma_i^2 : i = 1, \dots, N_h^2\}$ are associated degrees of freedom (i.e., dual bases of linear forms) defined on $\mathbf{H}_0(\text{curl})$ and L^2 , respectively.

Denoting \mathcal{E}^n , $\mathcal{B}^{n+1/2}$ the column vectors containing the coefficients of \mathbf{E}_h^n and $B_h^{n+1/2}$ in Φ_h^1 and Ψ_h^2 , the matrix formulation of (26)-(27) reads

$$M_1(\mathcal{E}^{n+1} - \mathcal{E}^n) - c^2 \Delta t R \mathcal{B}^{n+1/2} = -\Delta t \varepsilon_0^{-1} \mathcal{J}^{n+1/2} \quad (35)$$

$$M_2(\mathcal{B}^{n+1/2} - \mathcal{B}^{n-1/2}) + \Delta t R^T \mathcal{E}^n = 0 \quad (36)$$

with

$$M_1 := \left(\int_{\Omega} \varphi_i^1 \cdot \varphi_j^1 \right)_{1 \leq i, j \leq N_h^1}, \quad M_2 := \left(\int_{\Omega} \psi_i^2 \psi_j^2 \right)_{1 \leq i, j \leq N_h^2} \quad \text{and} \quad R := \left(\int_{\Omega} \psi_j^2 \text{curl} \varphi_i^1 \right)_{\substack{1 \leq i \leq N_h^1 \\ 1 \leq j \leq N_h^2}}$$

denote respectively the mass matrices of Φ_h^1 , Ψ_h^2 and the associated (rectangular) curl matrix, and where $\mathcal{J}^{n+1/2}$ is the discrete current vector which components are given by

$$\mathcal{J}_i^{n+1/2} := \int_{\Omega} \mathbf{J}_h^{n+1/2} \cdot \varphi_i^1, \quad 1 \leq i \leq N_h^1.$$

Remark 5.1 *According to the exact sequence (21), it is possible to derive another expression for the matrix R which simplifies (36). Indeed, since $\text{curl} \varphi_i^1 \in V_h^2$ for any basis function of \mathbf{V}_h^1 , one may decompose $\text{curl} \varphi_i^1 = \sum_{\ell=1}^{N_h^2} \sigma_{\ell}^2 (\text{curl} \varphi_i^1) \psi_{\ell}^2$. It follows that R reads*

$$R = K M_2 \quad \text{with} \quad K := (\sigma_{\ell}^2 (\text{curl} \varphi_i^1))_{1 \leq i \leq N_h^1, 1 \leq \ell \leq N_h^2}$$

and because M_2 , as a mass matrix, is s.p.d., (35)-(36) can be equivalently rewritten into

$$M_1(\mathcal{E}^{n+1} - \mathcal{E}^n) - c^2 \Delta t K M_2 \mathcal{B}^{n+1/2} = -\Delta t \varepsilon_0^{-1} \mathcal{J}^{n+1/2} \quad (37)$$

$$(\mathcal{B}^{n+1/2} - \mathcal{B}^{n-1/2}) + \Delta t K^T \mathcal{E}^n = 0. \quad (38)$$

Note that the discrete Faraday law is now fully explicit, independently of the basis chosen for V_h^2 . Moreover this corresponds to formulations based on discrete differential forms, the matrices M_1 and M_2 representing the discrete Hodge operators, see [7] for more details.

Let us end this section by observing that one last version of the “charge conservation theorem” – completely equivalent with Theorem 4.1 – can be given, based on the above matrix formulation. To that purpose, consider that $\Phi_h := \{\phi_i^0 : i = 1, \dots, N_h^0\}$ is a basis of V_h^0 , and introduce

$$A := \left(- \int_{\Omega} \varphi_j^1 \cdot \mathbf{grad} \phi_i^0 \right)_{\substack{1 \leq i \leq N_h^0 \\ 1 \leq j \leq N_h^1}} \quad \text{and} \quad \mathcal{R}^n := \left(\int_{\Omega} \rho_h^n \phi_i^0 \right)_{1 \leq i \leq N_h^0}.$$

Then we have the following result.

Theorem 5.1 (charge conservation – fully discrete level in matrix form) *Given the discrete Ampere law in matrix form (35), the following are equivalent:*

(i) *the fully discrete Gauss law in matrix form*

$$A\mathcal{E}^n = \varepsilon_0^{-1}\mathcal{R}^n \quad (39)$$

holds at any time step n ,

(ii) *the discrete Gauss law (39) holds at the initial time step $n = 0$ only, and the source vectors $\mathcal{R}^n, \mathcal{J}^{n+1/2}$ satisfy the following discrete charge conservation property:*

$$\mathcal{R}^{n+1} - \mathcal{R}^n + \Delta t G \mathcal{J}^{n+1/2} = 0 \quad \forall n \in \mathbb{N}, \quad (40)$$

where G is the rectangular matrix given by $G_{i,j} := -\sigma_j^1(\mathbf{grad} \phi_i^0)$, $1 \leq i \leq N_h^0$, $1 \leq j \leq N_h^1$.

Proof. Of course we do not need a proof for this statement, since it is nothing but the matrix form of Theorem 4.1. But observe that a direct argument can be written as follows: from $\mathbf{grad}(V_h^0) \subset \mathbf{V}_h^1$, we have $\mathbf{grad}(\phi_i^0) = \sum_{j=1}^{N_h^1} \sigma_j^1(\mathbf{grad}(\phi_i^0))\varphi_j^1$ for any i , hence $A = GM_1$. In particular, multiplying Ampere’s law (35) by G yields

$$A(\mathcal{E}^{n+1} - \mathcal{E}^n) = -\Delta t \varepsilon_0^{-1} G \mathcal{J}^{n+1/2}, \quad (41)$$

where again we have used the fact that the curl of a gradient always vanishes, and more precisely,

$$(GR)_{i,j} = - \sum_{k=1}^{N_h^1} \left(\sigma_k^1(\mathbf{grad} \phi_i^0) \int_{\Omega} \psi_j^2 \operatorname{curl} \varphi_k^1 \right) = - \int_{\Omega} \psi_j^2 \operatorname{curl}(\mathbf{grad} \phi_i^0) = 0. \quad (42)$$

The desired result follows then easily from (41). ■

5.2 Computing the new discrete current

Let us now give a simple and practical algorithm to compute the new (consistent) right hand side $\mathcal{J}^{n+1/2}$ appearing in the matrix formulation (35)-(36) of the FE Maxwell solver. Here we restrict to the simpler case *without regularization* where $S = \delta$. In this case, indeed, the usual coupling (28) classically leads to a discrete current given by

$$\mathcal{J}_i^{n+1/2} := \int_{\Omega} \mathbf{J}_h^{n+1/2} \cdot \varphi_i^1 = \sum_{k=1}^{N_{\text{part}}} w_k \mathbf{v}_k^{n+1/2} \cdot \int_{\Omega} \delta(\mathbf{x} - \mathbf{x}_k^{n+1/2}) \varphi_i^1(\mathbf{x}) \, d\mathbf{x} = \sum_{k=1}^{N_{\text{part}}} w_k \mathbf{v}_k^{n+1/2} \cdot \varphi_i^1(\mathbf{x}_k^{n+1/2}) \quad (43)$$

for $i = 1, \dots, N_h^1$, whereas the consistent coupling (33) yields

$$\mathcal{J}_i^{n+\frac{1}{2}} := \int_{\Omega} \mathbf{J}_h^{n+\frac{1}{2}} \cdot \boldsymbol{\varphi}_i^1 = \frac{1}{\Delta t} \sum_{k=1}^{N_{\text{part}}} \mathbf{v}_k^{n+\frac{1}{2}} \cdot \int_{t_n}^{t_{n+1}} \boldsymbol{\varphi}_i^1(\mathbf{x}_k(t)) dt \quad (44)$$

with $\mathbf{x}_k(t) := \mathbf{x}_k^n + (t - t_n)\mathbf{v}_k^{n+\frac{1}{2}}$ on $[t_n, t_{n+1}]$. Note that the right hand side of the Maxwell solver is now well defined even in the case where the particles are located on the edges of the FE mesh, compare with Remark 4.1. Now, even though that formula may seem rather involved compared to the former one, it is possible to compute it exactly with almost no additional implementation costs. Indeed, every trajectory \mathbf{x}_k being affine on $[t_n, t_{n+1}]$, we easily infer from the piecewise polynomial structure of $\boldsymbol{\varphi}_i^1$ that if \mathbf{x}_k stays within a cell κ during a sub-interval $[\tau, \tau + \Delta\tau]$ of $[t_n, t_{n+1}]$, the function $t \rightarrow \boldsymbol{\varphi}_i^1(\mathbf{x}_k(t))$ is a univariate polynomial on that interval. More precisely, in the case of the structured finite element spaces (19), every piece $\boldsymbol{\varphi}_i^1|_{\kappa}$ is in $\mathbb{Q}_{p-1,p} \times \mathbb{Q}_{p,p-1}$ therefore

$$t \rightarrow \boldsymbol{\varphi}_i^1(\mathbf{x}_k(t)) \in (\mathbb{P}_{2p-1})^2 \quad \text{on } [\tau, \tau + \Delta\tau].$$

For spaces (20) defined on general triangulations, every piece $\boldsymbol{\varphi}_i^1|_{\kappa}$ is in $(\mathbb{P}_p)^2$, and hence

$$t \rightarrow \boldsymbol{\varphi}_i^1(\mathbf{x}_k(t)) \in (\mathbb{P}_p)^2 \quad \text{on } [\tau, \tau + \Delta\tau].$$

In particular, a Gauss-Legendre quadrature formula with respectively p or $\lceil \frac{p+1}{2} \rceil$ points on $[\tau, \tau + \Delta\tau]$ will be exact for the associated integral, i.e., we have

$$\int_{\tau}^{\tau+\Delta\tau} \boldsymbol{\varphi}_i^1(\mathbf{x}_k(t)) dt = \frac{\Delta\tau}{2} \sum_{j=1}^{p'} \lambda_{p',j} \boldsymbol{\varphi}_i^1 \left(\mathbf{x}_k(\tau) + \frac{(s_{p',j} + 1)\Delta\tau}{2} \mathbf{v}_k^{n+\frac{1}{2}} \right), \quad (45)$$

with $p' = p$ or $\lceil \frac{p+1}{2} \rceil$ depending whether the cell κ is a quadrangle or a triangle. Here $\lambda_{p',i}$ and $s_{p',i}$ denote the Gauss-Legendre weights and points corresponding to the reference interval $[-1, 1]$, which we recall below for $p' \leq 5$. To explicitly compute the discrete current vector $\mathcal{J}^{n+\frac{1}{2}}$, it thus remains to track the cells travelled by every particle k , apply (45) on every such cell (once per basis function $\boldsymbol{\varphi}_i^1$ which support intersects this cell), and sum the contributions according to (44).

In particular, the resulting code essentially consists in point-wise evaluations of the basis functions $\boldsymbol{\varphi}_i^1$, as is the case with the usual formula (43). Let us summarize it for the sake of clarity.

Algorithm 5.2 (computation of the current vector $\mathcal{J}^{n+1/2}$)

1. set $\mathbf{J_tmp}[i] := 0$ for all $i \in \{1, \dots, N_h^1\}$
2. for $k = 1, \dots, N_{\text{part}}$, do {
 - (a) set $\tau := t_n$, and let κ be the cell containing $\mathbf{x}_k(\tau + 0^+)$
 - (b) while $\left\{ \Delta\tau := \sup \{ \theta \in [0, t_{n+1} - \tau] : \mathbf{x}_k(\tau + \theta) \in \kappa \} > 0 \right\}$, do {
 - i. for any $i \in \{1, \dots, N_h^1\}$ such that $\text{supp}(\boldsymbol{\varphi}_i^1) \cap \kappa \neq \emptyset$, set

$$\mathbf{J_tmp}[i] := \mathbf{J_tmp}[i] + \frac{\Delta\tau}{2\Delta t} \mathbf{v}_k^{n+\frac{1}{2}} \cdot \sum_{j=1}^{p'} \lambda_{p',j} \boldsymbol{\varphi}_i^1 \left(\mathbf{x}_k(\tau) + \frac{(s_{p',j} + 1)\Delta\tau}{2} \mathbf{v}_k^{n+\frac{1}{2}} \right),$$

- ii. set $\tau := \tau + \Delta\tau$, and let κ be the cell containing $\mathbf{x}_k(\tau + 0^+)$

p'	$\{s_{p',j} : j = 1, \dots, p'\}$	$\{\lambda_{p',j} : j = 1, \dots, p'\}$
1	0	2
2	$\pm \frac{1}{3}\sqrt{3} \approx \pm 0.57735$	1
3	0	$\frac{8}{9} \approx 0.888889$
	$\pm \frac{1}{5}\sqrt{15} \approx \pm 0.774597$	$\frac{5}{9} \approx 0.555556$
4	$\pm \frac{1}{35}\sqrt{525 - 70\sqrt{30}} \approx \pm 0.339981$	$\frac{1}{36}(18 + \sqrt{30}) \approx 0.652145$
	$\pm \frac{1}{35}\sqrt{525 + 70\sqrt{30}} \approx \pm 0.861136$	$\frac{1}{36}(18 - \sqrt{30}) \approx 0.347855$
5	0	$\frac{128}{225} \approx 0.568889$
	$\pm \frac{1}{21}\sqrt{245 - 14\sqrt{70}} \approx \pm 0.538469$	$\frac{1}{900}(322 + 13\sqrt{70}) \approx 0.478629$
	$\pm \frac{1}{21}\sqrt{245 + 14\sqrt{70}} \approx \pm 0.90618$	$\frac{1}{900}(322 - 13\sqrt{70}) \approx 0.236927$

Table 1: Reference Gauss-Legendre nodes and weights for $p' \leq 5$.

}

3. set $\mathcal{J}_i^{n+1/2} := \text{J_tmp}[i]$

Remark 5.3 *Since the time integral is always one-dimensional, the above algorithm is valid for all kind of piecewise polynomial elements (i.e., for all geometries, orders and dimensions), as long as the number of nodes p' is chosen accordingly.*

5.3 Mass lumping on structured meshes

Here we recall one basis proposed by Cohen and Monk in [9] for the curl-conforming Nédélec space \mathbf{V}_h^1 in the case of a structured mesh, which allows to lump the Mass matrix M_1 arising in the finite element method, see Section 5.1. As was mentioned in (19), the space \mathbf{V}_h^1 consists in this case of functions which restrictions to any cell $\kappa_{i,j} = [ih, (i+1)h] \times [jh, (j+1)h] \in \Omega_h$ are polynomials of $\mathbb{Q}_{p-1,p} \times \mathbb{Q}_{p,p-1}$. In order to characterize the basis functions, the degrees of freedom are defined as follows. We first denote by

$$0 < \hat{\nu}_1 < \dots < \hat{\nu}_a < \dots < \hat{\nu}_p < 1 \quad \text{and} \quad 0 = \hat{\nu}_{0,0} < \dots < \hat{\nu}_{0,b} < \dots < \hat{\nu}_{0,p} = 1$$

the Gauss-Legendre and Gauss-Lobatto nodes on the reference interval $[0, 1]$, and next define the $2p(p+1) = \dim(\mathbb{Q}_{p-1,p} \times \mathbb{Q}_{p,p-1})$ associated bivariate nodes in the reference quadrangle $[0, 1]^2$ by

$$\hat{m}_{(x,a,b)} := (\hat{\nu}_a, \hat{\nu}_{0,b}) \quad \text{and} \quad \hat{m}_{(y,a,b)} := (\hat{\nu}_{0,b}, \hat{\nu}_a) \quad \text{for} \quad a = 1, \dots, p, \quad b = 0, \dots, p. \quad (46)$$

The associated (reference) degrees of freedom are then given by

$$\hat{\sigma}_{(\xi,a,b)}^1(\mathbf{v}) = (\mathbf{v} \cdot \boldsymbol{\tau}_\xi)(\hat{m}_{(\xi,a,b)}), \quad \xi = x \text{ or } y, \quad a = 1, \dots, p, \quad b = 0, \dots, p, \quad (47)$$

where $\boldsymbol{\tau}_x := \begin{pmatrix} 1 \\ 0 \end{pmatrix}$ and $\boldsymbol{\tau}_y := \begin{pmatrix} 0 \\ 1 \end{pmatrix}$ denote the unit vectors tangent to the axes. As it can be easily checked, these linear forms are independent on $\mathbb{Q}_{p-1,p} \times \mathbb{Q}_{p,p-1}$, hence there exists a unique basis

$\{\hat{\varphi}_{(\xi,a,b)}^1 : \xi = x \text{ or } y, a = 1, \dots, p, b = 0, \dots, p\}$ of $\mathbb{Q}_{p-1,p} \times \mathbb{Q}_{p,p-1}$, characterized by the relations $\hat{\sigma}_\lambda^1(\hat{\varphi}_\mu^1) = \delta_{\lambda,\mu}$. The corresponding functions are given by

$$\hat{\varphi}_{(x,a,b)}^1(x,y) := \begin{pmatrix} L_a(x)L_{0,b}(y) \\ 0 \end{pmatrix} \quad \text{and} \quad \hat{\varphi}_{(y,a,b)}^1(x,y) := \begin{pmatrix} 0 \\ L_a(y)L_{0,b}(x) \end{pmatrix} \quad (48)$$

for $a = 1, \dots, p$ and $b = 0, \dots, p$. Here L_a and $L_{0,b}$ denote the univariate Lagrange polynomials of degree $p-1$ and p associated with the nodes \hat{v}_i and $\hat{v}_{0,j}$, respectively. It is then possible to define a curl-conforming basis of \mathbf{V}_h^1 by appropriately transporting these functions and degrees of freedom on every quadrangle κ of Ω_h . More precisely, we first transport the reference nodes as $m_{(\xi,a,b)}^{\kappa_{i,j}} := \hat{m}_{\xi,a,b} + (ih, jh)$, and associated with interior nodes, set

$$\varphi_\lambda^1(x,y) := \hat{\varphi}_{\xi,a,b}^1\left(\frac{x-ih}{h}, \frac{y-jh}{h}\right) \quad \text{for} \quad \lambda = (\kappa_{i,j}, \xi, a, b) \quad \text{such that} \quad 1 \leq b \leq p-1.$$

Because of the curl-conformity, basis functions associated with boundary nodes (i.e., such that $b = 0$ or p) are obtained by stitching together two pieces coming from adjacent cells: for instance,

$$\varphi_{\kappa_{i,j},x,a,0}^1(x,y) := \hat{\varphi}_{x,a,0}^1\left(\frac{x-ih}{h}, \frac{y-jh}{h}\right) + \hat{\varphi}_{x,a,p}^1\left(\frac{x-ih}{h}, \frac{y-(j-1)h}{h}\right)$$

is associated with $m_{(x,a,0)}^{\kappa_{i,j}} = m_{(x,a,p)}^{\kappa_{i,j-1}}$, and so forth.

Finally, the associated mass matrix M_1 can be lumped by approximating the L^2 scalar product with quadrature formulas involving the univariate Gauss-Legendre and Gauss-Lobatto nodes as follows. Denote by λ_i and $\lambda_{0,j}$ are the corresponding weights on the interval $[0, 1]$, then set

$$\langle \mathbf{u}, \mathbf{v} \rangle_{*,\kappa} := h^2 \sum_{i=1}^p \sum_{j=0}^p \lambda_i \lambda_{0,j} (u_x v_x(m_{(x,i,j)}^\kappa) + u_y v_y(m_{(y,i,j)}^\kappa)) \approx \int_\kappa \mathbf{u} \cdot \mathbf{v}$$

and finally

$$\langle \mathbf{u}, \mathbf{v} \rangle_{*,h} := \sum_{\kappa \in \Omega_h} \langle \mathbf{u}, \mathbf{v} \rangle_{*,\kappa} \approx \int_\Omega \mathbf{u} \cdot \mathbf{v}.$$

This yields an admissible approximation for the mass matrix (a dispersion analysis is given in [9]), and by observing that the restriction of any basis function φ_λ^1 to some cell of Ω_h coincides with one suitably transported reference basis function $\hat{\varphi}_{(\xi,i,j)}^1$, it is easily checked that the resulting matrix, which entries read $(M_{1,*})_{\lambda,\gamma} := \langle \varphi_\lambda^1, \varphi_\gamma^1 \rangle_{*,h}$, is indeed diagonal.

5.4 Comparison with the Villasenor-Buneman scheme

Let us now observe that our formulation applied to the above lumped elements (in the first order case, i.e., with $p = 1$) is equivalent to the charge conserving method of Villasenor and Buneman coupled to Yee's solver for the Maxwell system.

In the first order case, the curl-conforming basis functions obtained by stitching together the polynomial pieces (48) correspond to products of the first two (univariate) B-splines rescaled at the cell size h , namely

$$S_h^0(x) := \mathbf{1}_{[0,1]}\left(\frac{x}{h}\right) \quad \text{and} \quad S_h^1(x) := \max\left\{1 - \left|\frac{x}{h}\right|, 0\right\}.$$

Indeed the reference nodes (46) are in this case

$$\hat{m}_{(x,1,0)} = \left(\frac{1}{2}, 0\right), \quad \hat{m}_{(x,1,1)} = \left(\frac{1}{2}, 1\right), \quad \hat{m}_{(y,1,0)} = \left(0, \frac{1}{2}\right) \quad \text{and} \quad \hat{m}_{(y,1,1)} = \left(1, \frac{1}{2}\right),$$

hence each global basis function is associated with a node

$$m_{i+\frac{1}{2},j} \equiv m_{(x,1,0)}^{\kappa_{i,j}} = m_{(x,1,1)}^{\kappa_{i,j-1}} := ((i+\frac{1}{2})h, jh) \quad \text{or} \quad m_{i,j+\frac{1}{2}} \equiv m_{(y,1,0)}^{\kappa_{i,j}} = m_{(y,1,1)}^{\kappa_{i-1,j}} := (ih, (j+\frac{1}{2})h)$$

together with the corresponding degree of freedom, see (47), and it reads

$$\varphi_{i+\frac{1}{2},j}^1(x,y) = \begin{pmatrix} S_h^0(x-ih)S_h^1(y-jh) \\ 0 \end{pmatrix} \quad \text{or} \quad \varphi_{i,j+\frac{1}{2}}^1(x,y) = \begin{pmatrix} 0 \\ S_h^1(x-ih)S_h^0(y-jh) \end{pmatrix}.$$

Note that due to the homogeneous boundary conditions, only the functions associated with nodes interior to Ω belong to \mathbf{V}_h^1 . As for the (reference) quadrature weights, we have $\lambda_1 = 1$ and $\lambda_{0,0} = \lambda_{0,1} = \frac{1}{2}$, therefore all diagonal terms of the (diagonal) lumped mass matrix $M_{1,*}$ are equal to h^2 . In order to write the resulting system (37)-(38), it now remains to calculate the matrices K and M_2 . To this purpose we define the basis functions of the L^2 conforming space V_h^2 as

$$\psi_{i+\frac{1}{2},j+\frac{1}{2}}^2(x,y) := S_h^0(x-ih)S_h^0(y-jh)$$

with degrees of freedom $\sigma_{i+\frac{1}{2},j+\frac{1}{2}}^2(v) := v((i+\frac{1}{2})h, (j+\frac{1}{2})h)$, According to $(S_h^1)' = \frac{1}{h}[S_h^0(\cdot+h) - S_h^0(\cdot)]$ we have

$$\text{curl } \varphi_{i+\frac{1}{2},j}^1 = -\partial_y(\varphi_{i+\frac{1}{2},j}^1)_x = -\frac{1}{h}S_h^0(x-ih)[S_h^0(y-(j-1)h) - S_h^0(y-jh)] = \frac{1}{h}(\psi_{i+\frac{1}{2},j+\frac{1}{2}}^2 - \psi_{i+\frac{1}{2},j-\frac{1}{2}}^2)$$

and similarly,

$$\text{curl } \varphi_{i,j+\frac{1}{2}}^1 = \partial_x(\varphi_{i,j+\frac{1}{2}}^1)_y = \frac{1}{h}S_h^0(y-jh)[S_h^0(x-(i-1)h) - S_h^0(x-ih)] = -\frac{1}{h}(\psi_{i+\frac{1}{2},j+\frac{1}{2}}^2 - \psi_{i-\frac{1}{2},j+\frac{1}{2}}^2)$$

It follows that every line of K contains two non-zero terms, namely

$$\sigma_{i+\frac{1}{2},j\pm\frac{1}{2}}^2(\text{curl } \varphi_{i+\frac{1}{2},j}^1) = \pm\frac{1}{h} \quad \text{and} \quad \sigma_{i\pm\frac{1}{2},j+\frac{1}{2}}^2(\text{curl } \varphi_{i,j+\frac{1}{2}}^1) = \mp\frac{1}{h}.$$

As for the mass matrix M_2 , it is clearly diagonal, with values $\int_{\Omega}(\psi_{i+\frac{1}{2},j+\frac{1}{2}}^2)^2 = h^2$. Hence the system (37)-(38) reads

$$\begin{aligned} \frac{1}{\Delta t}(\mathcal{E}_x^{n+1} - \mathcal{E}_x^n)_{i+\frac{1}{2},j} - \frac{c^2}{h}[(\mathcal{B}_z^{n+\frac{1}{2}})_{i+\frac{1}{2},j+\frac{1}{2}} - (\mathcal{B}_z^{n+\frac{1}{2}})_{i+\frac{1}{2},j-\frac{1}{2}}] &= (\mathcal{J}_x^{n+\frac{1}{2}})_{i+\frac{1}{2},j} \\ \frac{1}{\Delta t}(\mathcal{E}_y^{n+1} - \mathcal{E}_y^n)_{i,j+\frac{1}{2}} + \frac{c^2}{h}[(\mathcal{B}_z^{n+\frac{1}{2}})_{i+\frac{1}{2},j+\frac{1}{2}} - (\mathcal{B}_z^{n+\frac{1}{2}})_{i-\frac{1}{2},j+\frac{1}{2}}] &= (\mathcal{J}_y^{n+\frac{1}{2}})_{i,j+\frac{1}{2}} \\ \frac{1}{\Delta t}(\mathcal{B}_z^{n+\frac{1}{2}} - \mathcal{B}_z^{n-\frac{1}{2}})_{i+\frac{1}{2},j+\frac{1}{2}} - \frac{1}{h}[(\mathcal{E}_x^n)_{i+\frac{1}{2},j+\frac{1}{2}} - (\mathcal{E}_x^n)_{i+\frac{1}{2},j} - (\mathcal{E}_y^n)_{i+1,j+\frac{1}{2}} + (\mathcal{E}_y^n)_{i,j+\frac{1}{2}}] &= 0 \end{aligned}$$

and we recognize the classical Yee scheme on staggered meshes (for simplicity we have written four \mathcal{E}^n terms in the third equation, but note that only those corresponding to interior nodes should appear, according to the structure of K).

Finally we observe that our consistent current source definition (33), i.e., (44) in the case without regularization, yields

$$(\mathcal{J}_x^{n+\frac{1}{2}})_{i+\frac{1}{2},j} = \frac{1}{\Delta t} \sum_{k=1}^{N_{\text{part}}} v_{k,x}^{n+\frac{1}{2}} \int_{t_n}^{t_{n+1}} S_h^0(x_k(t) - ih)S_h^1(y_k(t) - jh) dt$$

and

$$(\mathcal{J}_y^{n+\frac{1}{2}})_{i,j+\frac{1}{2}} = \frac{1}{\Delta t} \sum_{k=1}^{N_{\text{part}}} v_{k,y}^{n+\frac{1}{2}} \int_{t_n}^{t_{n+1}} S_h^1(x_k(t) - ih)S_h^0(y_k(t) - jh) dt,$$

which is exactly the charge conserving expression of Villasenor and Buneman, see [26].

6 Numerical experiments

6.1 Beam test case

Here we consider a rectangular domain $\Omega = [-5, 5] \times [-2.5, 2.5]$ with boundary conditions of absorbing Silver-Müller type on $|y| = 2.5$, and of perfect electric conductor type on $|x| = 5$. Particles of uniform (low) velocity along the direction x are injected into the domain near the left boundary $x = -5$, and then subject to a strong exterior electric field \mathcal{E}^{ext} also directed along the direction x .

We have implemented finite elements of second order ($p = 2$) corresponding to the spaces (20), using the unstructured mesh represented in Figure 2, left. In Figure 2, right we have represented the velocity of the particles with respect to their position, at a time when the first particles have reached the right boundary $x = 2.5$, and in Figure 3 we have represented the electric and magnetic fields at the same time. Notice that the magnetic field is discontinuous at the interface between cells and the electric field has a continuous tangential component and discontinuous normal component. However because the current is integrated along the whole trajectory of each particle these discontinuities do not degrade the solution. Here the asymmetry in the velocity corresponds to a slight expansion of the beam and already suggests a proper computation of the sources, indeed a lack of charge conservation usually results in an unphysical beam shrinkage, see e.g. the numerical experiments displayed in [4].

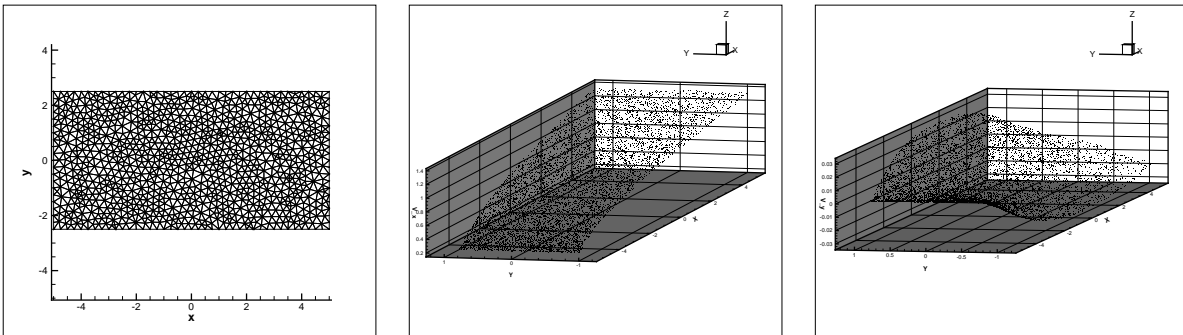


Figure 2: mesh used for the beam test case (left), and x and y components of the particles' velocity, with respect to their positions.

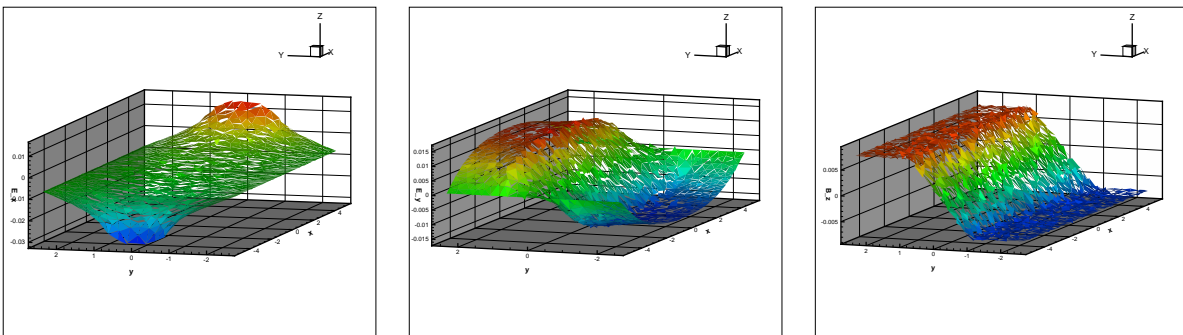


Figure 3: self consistent electric (x and y components) and magnetic field (right) at the same time than Figure 2.

More specifically, we note that the discrete Gauss law (39) is satisfied at the initial time (since

the initial charge density is zero and the initial electric field is uniform), and by computing the difference $A\mathcal{E}^n - \varepsilon_0^{-1}\mathcal{R}^n$ we have checked that it is also verified at any time step, as Theorem 4.2 claims.

6.2 Landau damping

The Landau damping problem is a purely electrostatic test case which strongly relies on Gauss' law being satisfied. In this test case, the initial density f_0 corresponds to a sinusoidal perturbation of a Maxwellian distribution with respect to velocity, i.e.,

$$f_0(\mathbf{x}, \mathbf{v}) := \frac{1}{2\pi} \left(1 + \epsilon \frac{\cos(\mathbf{k} \cdot \mathbf{x})}{2} \right) e^{-\frac{\mathbf{v}^2}{2}}$$

and is approximated by an initial distribution $f_h^0 := \sum_{k=1}^{N_{\text{part}}} \omega_k \delta(\mathbf{x} - \mathbf{x}_k^0, \mathbf{v} - \mathbf{v}_k^0)$ of weighted macro-particles, as described in Section 4. The resulting bunch of macro-particles is plotted – in the phase space – in Figure 4. Now, because the corresponding charge density ρ_h^0 is not uniformly zero (as in the previous test case), it is necessary to solve a Poisson problem:

$$\text{find } \Phi_h^0 \in H_0^1(\Omega) \quad \text{such that} \quad \Delta \Phi_h^0 = \frac{1}{\varepsilon_0} \rho_h^0$$

in order to determine a consistent initial electric field

$$\mathbf{E}_h^0 := -\mathbf{grad} \Phi_h^0 \tag{49}$$

that satisfies Gauss' law at time $t = 0$. Note that according to (33), the charge density ρ_h^0 is obtained by integrating f_h^0 with respect to velocity, hence if no regularization is performed it is not an L^2 (nor H^{-1}) function. Nevertheless, by using similar arguments as in Remark 4.3 we see that the above Poisson problem still makes sense when interpreted with the (continuous) test functions of V_h^0 , i.e., there is a unique $\Phi_h^0 \in V_h^0$ such that

$$-\int_{\Omega} \mathbf{grad} \Phi_h^0 \cdot \mathbf{grad} \phi = \frac{1}{\varepsilon_0} \sum_{k=1}^{N_{\text{part}}} \omega_k \phi(\mathbf{x}_k^0) \quad \forall \phi \in V_h^0,$$

and we can actually compute it by inverting the stiffness matrix of (any given basis of) V_h^0 . It is then readily seen that the field (49) is in \mathbf{V}_h^1 and satisfies the appropriate discrete Gauss' law, see (29) and Remark 4.1. And again, we have checked that the discrete Gauss law (39) is verified at any further time step. The resulting (continuous) potential Φ_h^0 and (curl-conforming) field \mathbf{E}_h^0 are plotted in Figure 5.

Finally we observe a correct behavior of the classical Landau damping test on Figure 6, which represents the time evolution of the norm of the electric field (in log scale).

7 Conclusion

We have developed a general charge conserving algorithm for electromagnetic PIC codes within the framework of Finite Element Maxwell solvers which are based on different discrete approximations for the electric and magnetic field which satisfy an exact sequence property. The setting can be used for arbitrary order finite elements on structured or unstructured grids of triangles and/or quadrilaterals. Within this framework, only Ampere's and Faraday's equations need to be solved numerically. A discrete version of Gauss's law is satisfied algebraically and up to machine accuracy in numerical experiments. This offers the possibility of using the recently developed high order highly accurate Maxwell solvers on structured and unstructured grids in the context of PIC plasma simulations which should be interesting for a wide range of applications.

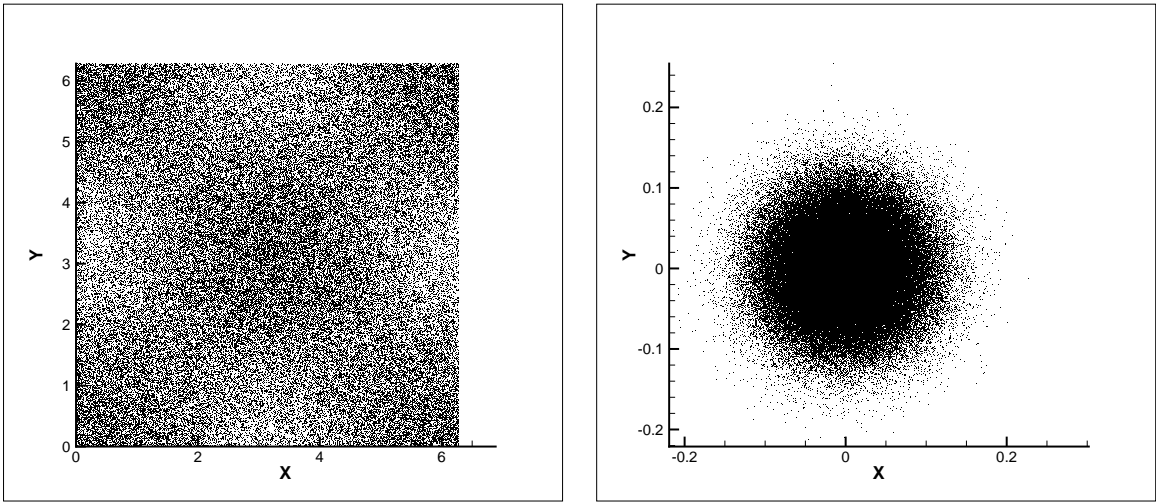


Figure 4: Initial distribution of macro-particles corresponding to f_h^0 , in \mathbf{x} (left) and \mathbf{v} (right).

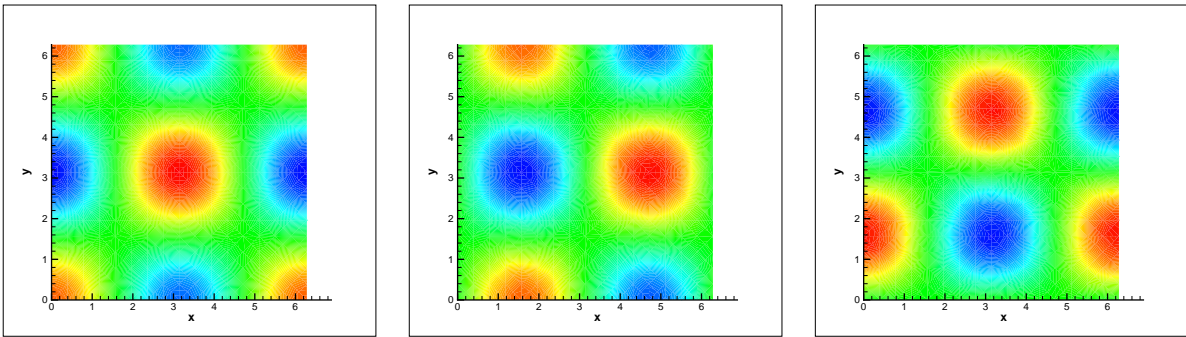


Figure 5: Scalar potential (left) and electric field corresponding to the initial density f_h^0 .

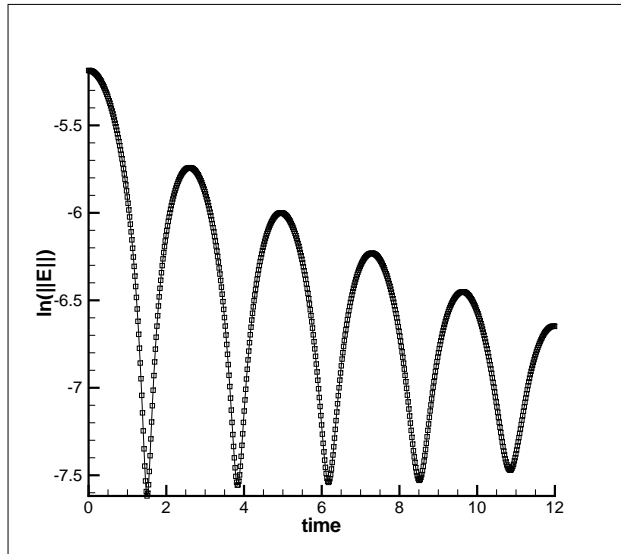


Figure 6: time evolution of the electric field (in log scale) for the Landau damping test case.

References

- [1] J. Adam, A. Serveniére, J.-C. Nédélec and P.-A. Raviart, Study of an implicit scheme for integrating Maxwell's equations, *Comput. Methods. Appl. Mech. Engrg.*, 22 (1980), no. 3, 327–346.
- [2] F. Assous, P. Degond, E. Heintze, P.-A. Raviart and J. Segre, On a finite-element method for solving the three-dimensional Maxwell equations, *J. Comput. Phys.* 109 (1993), no. 2, 222–237.
- [3] R. Barthelmé, P. Ciarlet, Jr. and E. Sonnendrücker, Generalized formulations of Maxwell's equations for numerical Vlasov-Maxwell simulations. *Math. Models Methods Appl. Sci.* 17 (2007), no. 5, 657–680.
- [4] R. Barthelmé and C. Parzani, Numerical charge conservation in particle-in-cell codes *Numerical methods for hyperbolic and kinetic problems, IRMA Lect. Math. Theor. Phys.* 7 (2005), 7–28.
- [5] C. K. Birdsall and A. B. Langdon, *Plasma physics via computer simulation*, Institute of Physics, Bristol, 1991.
- [6] J. P. Boris, Relativistic plasma simulations : Optimization of a hybrid code, in Proc. 4th Conf. Num. Sim. Plasmas (NRL Washington, 1970), pp. 3–67.
- [7] A. Bossavit, *Computational electromagnetism. Variational formulations, complementarity, edge elements.*, Academic Press, Inc., San Diego, CA, 1998.
- [8] P. Castillo, R. Rieben, D. White. FEMSTER: an object oriented class library of high-order discrete differential forms. *ACM Trans. Math. Softw.* 31 (4), 2005.
- [9] G. Cohen, P. Monk, Gauss point mass lumping schemes for Maxwell's equations. *Numer. Methods Partial Differential Equations* 14 (1998), no. 1, 63–88.
- [10] G.-H. Cottet and P.-A. Raviart, Particle methods for the one-dimensional Vlasov-Poisson equations. *SIAM J. Numer. Anal.* 21 (1984), 52–76.
- [11] R. Dautray and J.-L. Lions, *Analyse mathématique et calcul numérique pour les sciences et les techniques*, Volume 5, Masson, 1985.
- [12] A. Elmkins, P. Joly, Edge finite elements and mass lumping for Maxwell's equations: the 3D case. *C. R. Acad. Sci. Paris Sér. I Math.* 325 (1997), no. 11, 1217–1222.
- [13] T. Zh. Esirkepov, Exact charge conservation scheme for Particle-in-Cell simulation with an arbitrary form-factor, *Comput. Phys. Comm.* 135 (2001) 144–153.
- [14] A. Fisher, R.N. Rieben, G. Rodrigue and D.A. White, A generalized mass lumping technique for vector finite-element solutions of the time-dependent Maxwell equations. *IEEE Trans. Antennas and Propagation* 53 (2005), no. 9, 2900–2910.
- [15] V. Girault and P.-A. Raviart, *Finite Element Methods for Navier-Stokes Equations. Theory and Algorithms*. Springer, Berlin, 1986.
- [16] R. Hiptmair, Finite elements in computational electromagnetism, *Acta Numerica* (2002), pp. 237–339.
- [17] A. B. Langdon, On enforcing Gauss' law in electromagnetic particle-in-cell codes, *Comput. Phys. Commun.* 70 (1992) 447–450.

- [18] B. Marder, A method for incorporating Gauss's law into electromagnetic PIC codes, *J. Comput. Phys.* 68 (1987) 48–55.
- [19] P. Monk, A mixed method for approximating Maxwell's equations. *SIAM. J. Numer. Anal.* 28 (1991), no. 6, 1610–1634.
- [20] C.-D. Munz, P. Omnes, R. Schneider, E. Sonnendrücker, U. Voss (2000) : *Divergence correction techniques for Maxwell solvers based on a hyperbolic model*, *J. Comput. Phys.* 161, no. 2, pp. 484-511.
- [21] J.-C. Nédélec, Mixed finite elements in \mathbb{R}^3 . *Numer. Math.* 35 (1980), no. 3, 315–341.
- [22] J.-C. Nédélec, A new family of mixed finite elements in \mathbb{R}^3 . *Numer. Math.* 50 (1986), no. 1, 57–81.
- [23] S. Pernet, X. Ferrieres, G. Cohen, High spatial order finite element method to solve Maxwell's equations in time domain. *IEEE Trans. Antennas and Propagation* 53 (2005), no. 9, 2889–2899.
- [24] G. Rodrigue, D. White. A vector finite element time-domain method for solving Maxwell's equation on unstructured hexaedral grids. *SIAM J. Sci. Comput.* 23 (2001), no. 3, 683–706.
- [25] T. Umeda, Y. Omura, T. Tominaga, H. Matsumoto, A new charge conservation method in electromagnetic particle-in-cell simulations, *Comput. Phys. Commun.* 2004, vol. 156, no1, pp. 73–85.
- [26] J. Villasenor and O. Buneman, Rigorous charge conservation for local electromagnetic field solvers. *Comput. Phys. Commun.* 69 (1992) 306–316.